Modeling of High-Signal Electrostriction. II

J von Cieminski

Sektion Physik, Martin-Luther-University Halle-Wittenberg, Halle, GDR

Z. Naturforsch. **45a**, 1095–1101 (1990); received May 8, 1990

The predictions obtained with a thermodynamical method are compared with experimental results. Several materials which pass a ferroelectric phase transition of first or second order are investigated. The predictions correspond well with the experimentaly determined qualitative and quantitative features as to the field and temperature dependence. Finally, extraordinary strain-field curves are predicted and proved.

Key words: Electromechanical properties, Electrostriction, Ferroelectrics, Thermodynamic, Phase transition.

1. Introduction

The subject of [1] was a thermodynamic approach to describe the electrostrictive high-signal behaviour with the help of an inverse function according to

$$E(S) = \pm \sqrt{\alpha S + \beta S^2 + \gamma S^3 + \mu S^4 + \nu S^5},$$

where the coefficients α, β etc. are exclusively determined by the thermodynamical coefficients C, ξ, and ζ as well as by the electrostrictive Q-coefficients, the Curie temperature T_c and the temperature.

Depending on the order of the phase transition a strikingly different evolution of the high-signal strain-field curves was predicted (represented in Fig. 5 of [1]).

The aim of the present paper is a comparison of these predictions with experimental results and a search for especially qualified materials. The performance of the applied method is described in [2, 3].

2. Experimental Results

The first set of samples is combined out of several PLZT ceramics which pass a so-called diffused phase transition (relaxor ferroelectrics) and posses a perovskite structure. Figure 1 shows a collection of high-signal strain-field curves obtained from differently doted PLZT ceramics. The complete set of loops is observable for each of the investigated samples if only the temperature is changed in the necessary range. The shown representation was chosen to demonstrate that the discussed behaviour is universally valid for this group of materials.

Although the transition is smeared over a broad temperature range, the observed high-signal strain-field curves correspond to the predicted ones of a first order phase transition. This confirms not only the estimations given in [1] but points to the intrinsic character of the phase transition in the sphere of the microregions ("Känzig regions" [4]).

Since materials with a perovskite structure are not uniaxial ferroelectrics, 90°-domain switching can appear and complicate the measured strain-field dependences. The main feature, however, especially outside the ferroelectric phase should be determined by the mechanism discussed here.

A popular material for checking theoretical predictions is $BaTiO_3$, which passes near 120 °C through a first order phase transition. The trouble with it is the large spread of the electrostrictive Q-coefficients given in the literature ($6.8 \cdot 10^{-2}$ m^4/C^2 [5], $7.5 \cdot 10^{-2}$ m^4/C^2 [6], $8 \cdot 10^{-2}$ m^4/C^2 [7], $10.5 \cdot 10^{-2}$ m^4/C^2 [8], $10.6 \cdot 10^{-2}$ m^4/C^2 [9], $24.3 \cdot 10^{-2}$ m^4/C^2 [10], $32.7 \cdot 10^{-2}$ m^4/C^2 [11]). From this point of view the proposed thermodynamical approach offers the possibility to determine which of the above-mentioned values is realistic.

Starting from a value of $Q_{33} = 10.55 \cdot 10^{-2}$ m^4/C^2 determined by Sheludev [9] and Pan et al. [8] and using the following set of thermodynamical coefficients:

$$C = 1.5 \cdot 10^5 \text{ K} \quad [12],$$
$$\xi = -5.5 \cdot 10^8 \text{ Vm}^5/\text{C}^3 \quad [13],$$
$$\zeta = 1.7 \cdot 10^{10} \text{ Vm}^9/\text{C}^5 \quad [13] \text{ and}$$
$$T_c = 115 \text{ °C} \quad (T_0 \approx 121 \text{ °C}) \quad [12],$$

Reprints requests to Dr. J. von Cieminski, Sektion Physik, Martin-Luther-University Halle-Wittenberg, Friedemann-Bach-Platz 6, Halle 4020, GDR.

0932-0784 / 90 / 0900-1095 $ 01.30/0. – Please order a reprint rather than making your own copy.

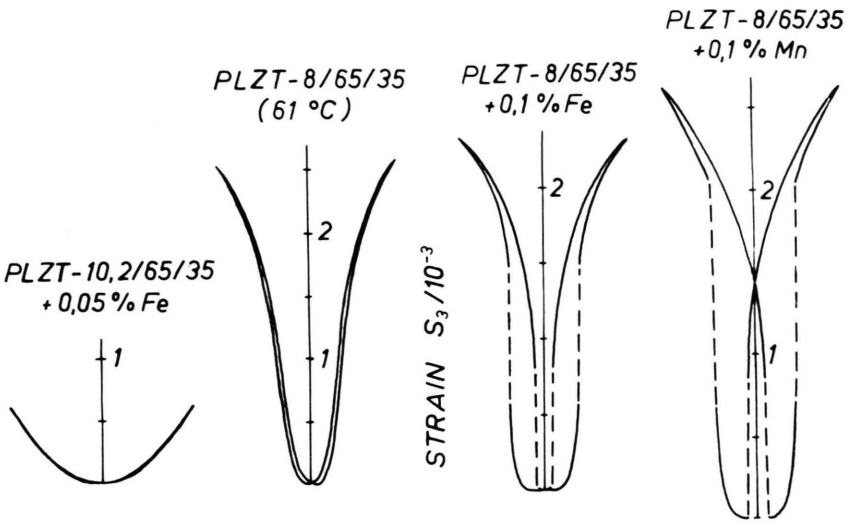

Fig. 1. High-signal strain-field curves of several PLZT ceramics (without specification the curves reflect the properties at room temperature; the maximum field strength is 15 kV/cm).

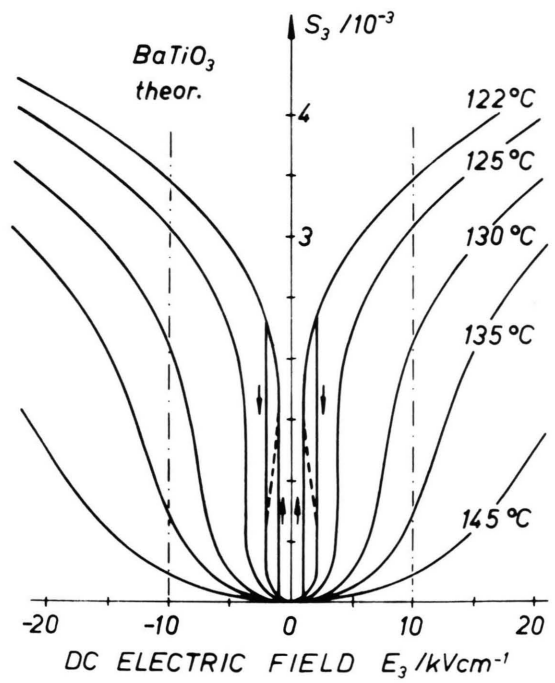

Fig. 2. Calculated high-signal strain-field curves of $BaTiO_3$ in the paraelectric phase.

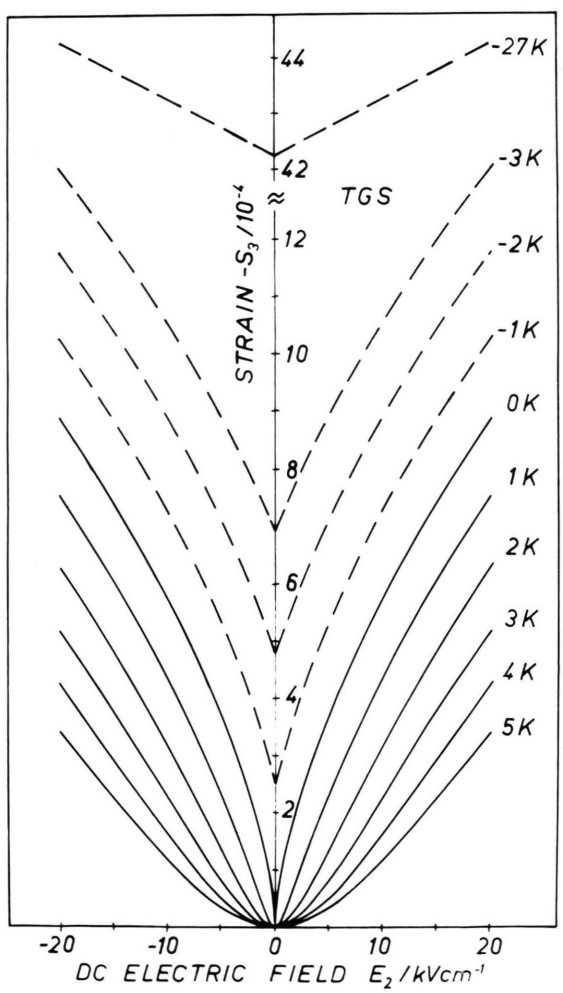

Fig. 3. Calculated transverse high-signal strain-field curves of TGS (the parameters correspond to the temperature difference $T - T_c$; $-S_3$ means a contraction).

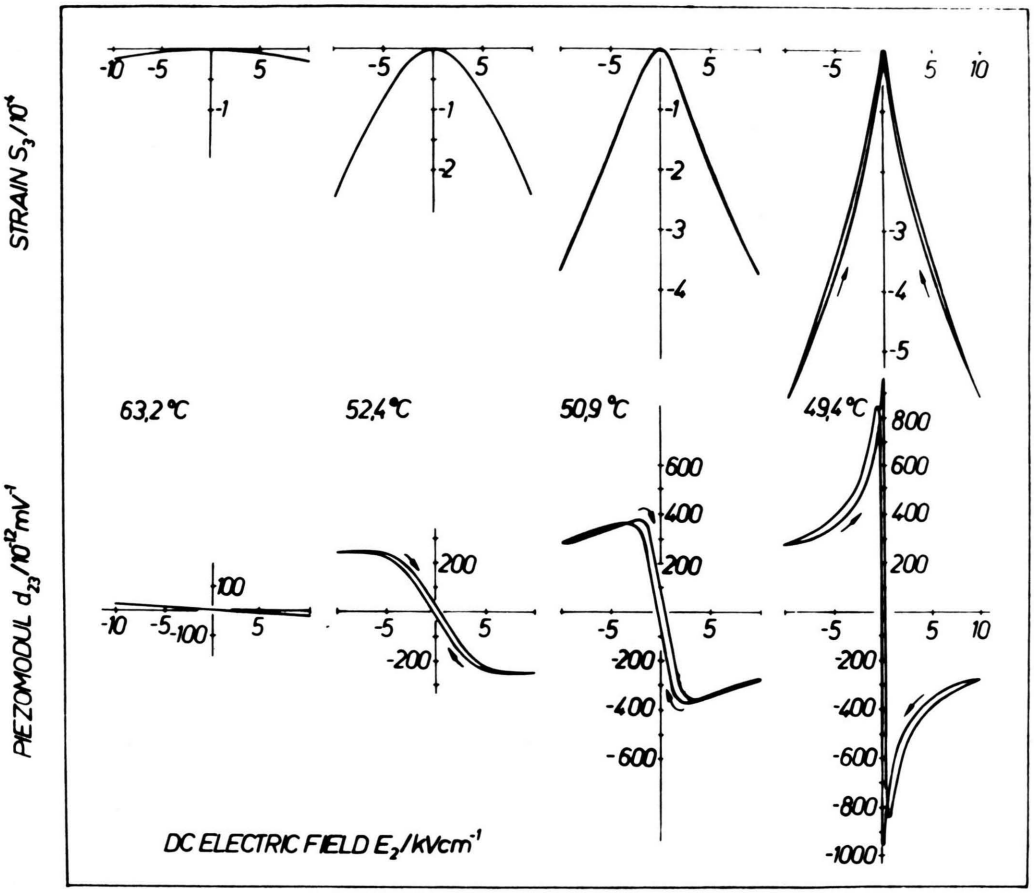

Fig. 4. Experimentally determined transverse high-signal strain-field curves and field dependences of the weak-signal piezomodul of TGS at different temperatures above T_c.

the calculations result in high-signal *S-E* dependences which are represented in Figure 2. These curves agree very well with the experimentally determined ones in least twinned crystals [8]. In such crystals 90°-domain switching is nearly excluded.

The predictions concerning a second order phase transition shall be examined by investigating TGS. Since it presents a uniaxial ferroelectric, 90°-domain switching is also excluded.

The calculations of the transverse high-signal electrostriction result in the curves presented in Figure 3. The following set of coefficients was used:

$Q_{23} = -4.45\ \mathrm{m^4/C^2}$ [14],
$C = 3190\ \mathrm{K}$ [15],
$\xi = 6.23 \cdot 10^{11}\ \mathrm{Vm^5/C^3}$ [16],
$\zeta = 4.02 \cdot 10^{14}\ \mathrm{Vm^9/C^5}$ [16] and
$T_c = 49.5\ ^\circ\mathrm{C}$.

It becomes obvious that near and some degrees below T_c the character of a root function must be expected, whereas a purely linear piezoelectric high-signal function should appear only clearly below T_c. Moreover, the fairly large maximum strain values at temperatures around T_c are also remarkable.

From the experiments result the curves presented in Figs. 4 and 5 in which also the field dependence of the weak-signal piezomodul is shown. The latter coincides rather well with the slope of the strain-field curve and indicates more clearly the field dependence of it. Obviously, the experimental results provide an excellent qualitative and quantitative confirmation of the predictions. Deviations are only observable within the ferroelectric phase and can be ascribed to the existence of surface layers or an internal bias.

In Figs. 6 and 7 the calculated strain-field dependences at three different temperatures and the pre-

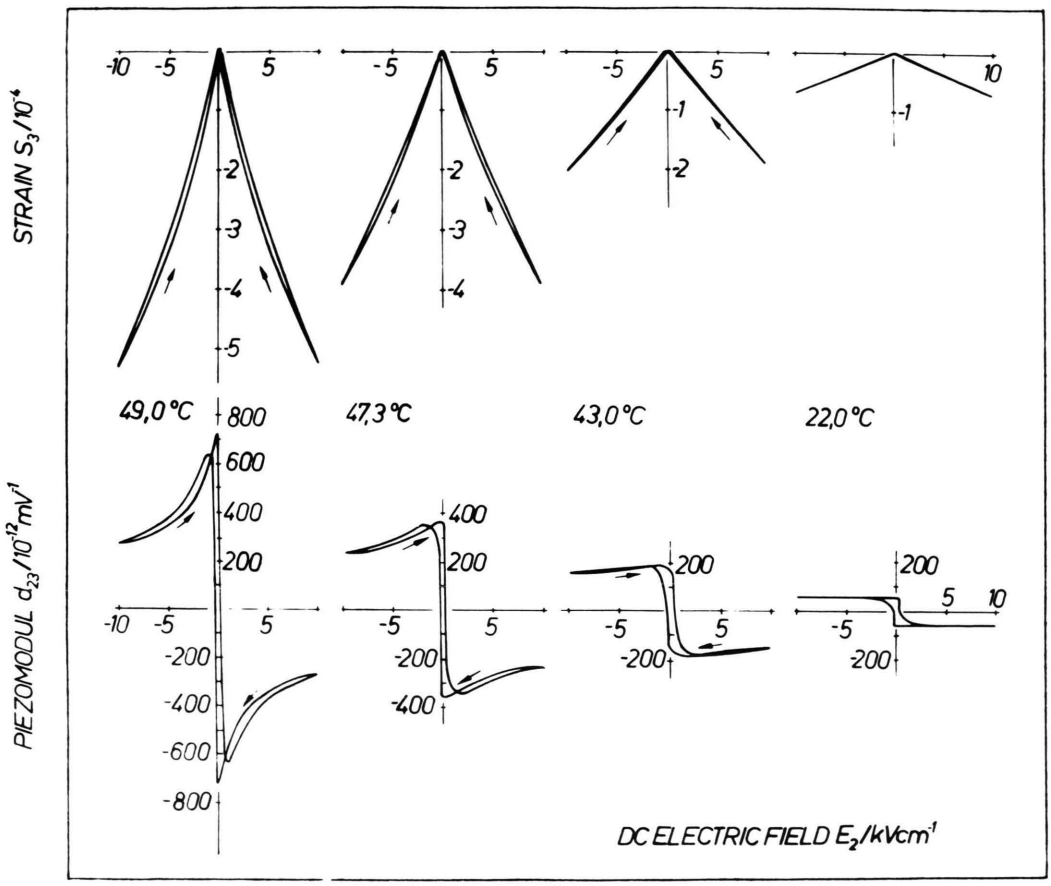

Fig. 5. Experimentally determined transverse high-signal strain-field curves and field dependences of the weak-signal piezomodul of TGS at different temperatures below T_c.

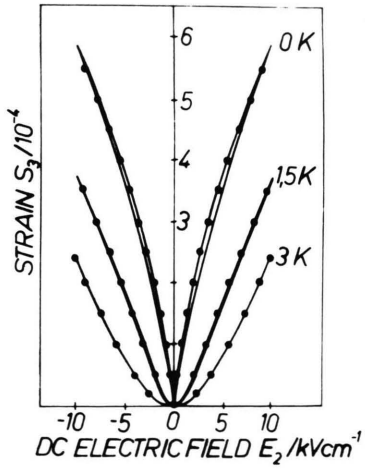

Fig. 6. Comparison of the calculated strain-field dependence of TGS (filled circles) with the experimental curves at three temperatures above T_c.

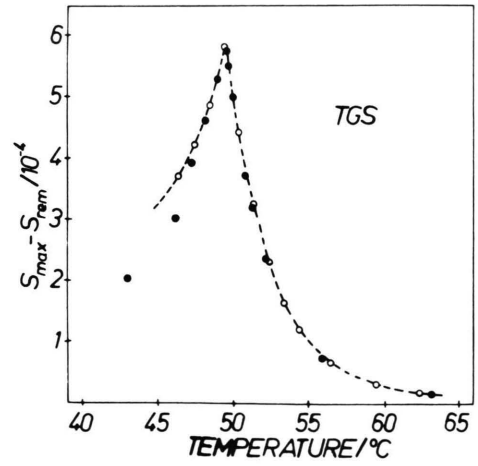

Fig. 7. Comparison of the predicted temperature dependence of the difference between the maximum strain value at 10 kV/cm and the remanent strain (open circles) with the experimental determined one (filled circles) of TGS.

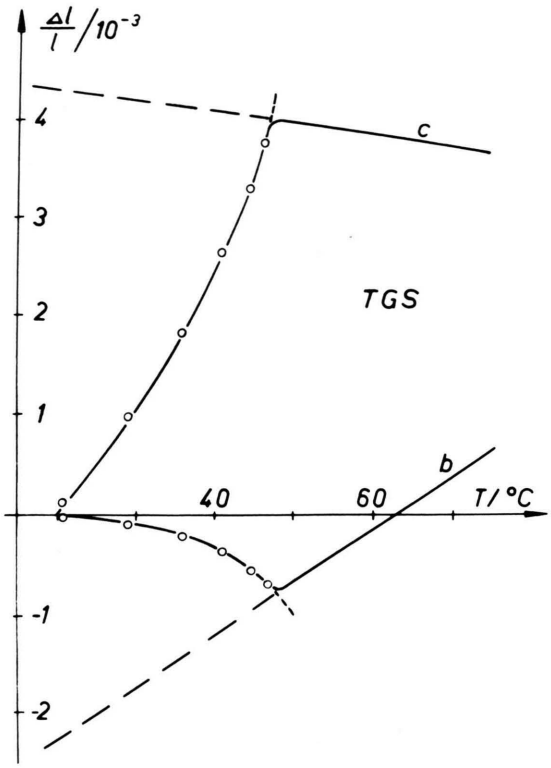

Fig. 8. Comparison of the calculated spontaneous strain of TGS at different temperatures (open circles) with the thermal expansion in the *b*- and *c*-direction (after [17]).

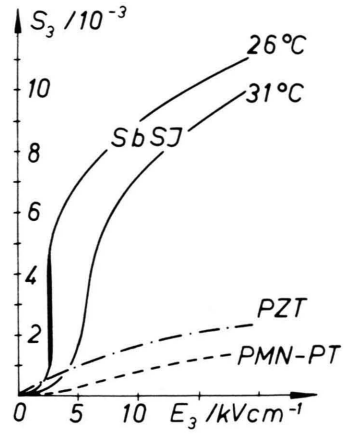

Fig. 9. Calculated high-signal strain-field curves of SbSI at two temperatures and the corresponding curves of PMN-PT and soft PZT ceramics at room temperature.

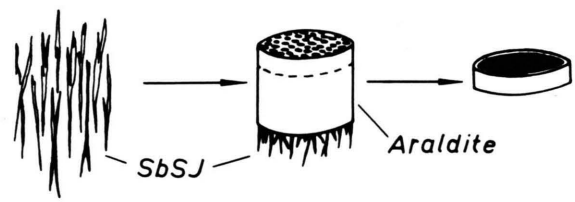

dicted temperature dependence of the maximum strain value at 10 kV/cm are compared with the experimental results. In Fig. 8 the predicted value of the spontaneous strain, determined by the remanent strain at zero field strength, are added to the linearly extrapolated values of the thermal expansion and compared with the experimental thermal expansion. In all cases a good agreement was found.

3. Predictions and New Applications

With three examples the expedience of the presented method shall be illustrated.

On looking for extraordinary strain-field dependences, the attention was drawn to the SbSI-group. Two representatives of this group – SbSI itself and BiSI – deserve a special attention.

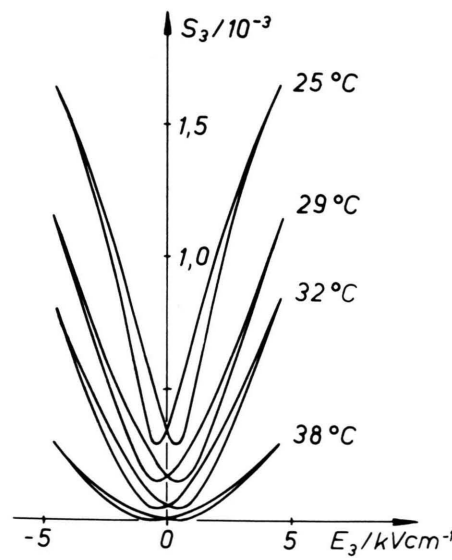

Fig. 10. Illustration of the preparation of the investigated SbSI-Araldite composite and the experimentally determined high-signal strain-field curves at different temperatures.

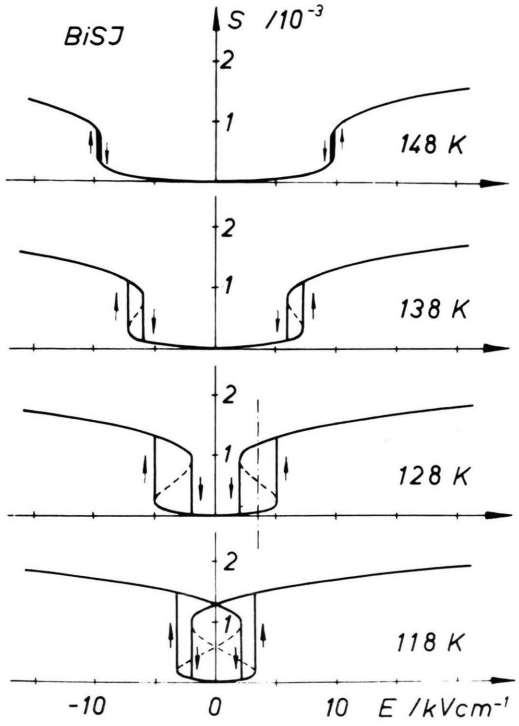

Fig. 11. Calculated high-signal strain-field curves of BiSI at different temperatures.

Using the following set of coefficients:

$Q_{33} = 19 \cdot 10^{-2}\ \mathrm{m^4/C^2}$ [18],

$C = 2.33 \cdot 10^5\ \mathrm{K}$ [19],

$\xi = -2.6 \cdot 10^8\ \mathrm{Vm^5/C^3}$ [20],

$\zeta = 5.4 \cdot 10^9\ \mathrm{Vm^9/C^5}$ [20] and

$T_c = 16\ ^\circ\mathrm{C}$ ($T_0 \approx 20\ ^\circ\mathrm{C}$) [20],

the calculations result in strain-field curves presented in Figure 9. Their special features are very large high-signal deformations which are five to ten times higher than those of Pb(Zr, Ti)O_3 (PZT) or $Pb(Mg_{1/3}Nb_{2/3})O_3$ (PMN) type ceramics.

The experimental examination is not too easy since SbSI was available only as thin needles (Figure 10). Therefore a composite of SbSI and Araldite (connectivity: 1–3) was investigated (cut and covered with electrodes as shown in Figure 10).

Of course, the observed curves cannot reach the predicted strain values of pure SbSI (more than 50% of the material consists of Araldite). But the realized ones (Fig. 10) are still very large (please note that the maximum field strength is only 5 kV/cm).

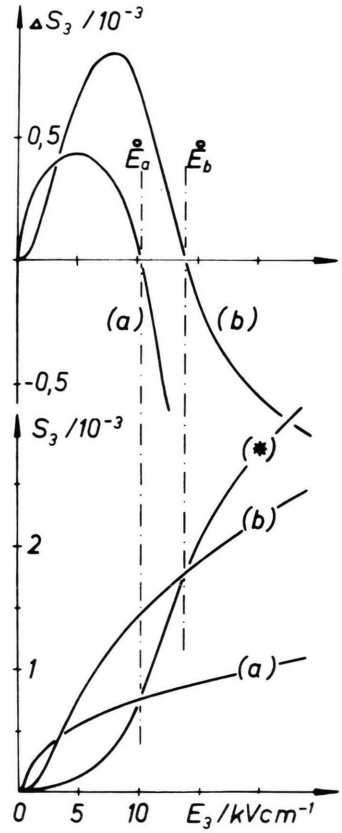

Fig. 12. Different strain-field dependences suited for the proposed bimorph combination and the corresponding deformation differences.

The second representative (BiSI) excels by particularly pronounced hysteresis (Figure 11). The used coefficients are:

$Q = 20 \cdot 10^{-2}\ \mathrm{m^4/C^2}$ (estimated),

$C = 1.9 \cdot 10^5\ \mathrm{K}$,

$\xi = -89 \cdot 10^8\ \mathrm{Vm^5/C^3}$,

$\zeta = 95 \cdot 10^{10}\ \mathrm{Vm^9/C^5}$ and

$T_c = 88\ \mathrm{K}$ ($T_0 \approx 113\ \mathrm{K}$),

determined by Pikka and Fridkin [20].

Here the predicted deformation jump is sufficiently high and the remaining field dependence relatively weak. Although an experimental examination could not be carried out, the calculations point to an interesting application of similar materials. Such strain-field dependences offer the possibility to use the material as a bistable longitudinal actuator (bistable electrostriction with on/off strain states). As proposed

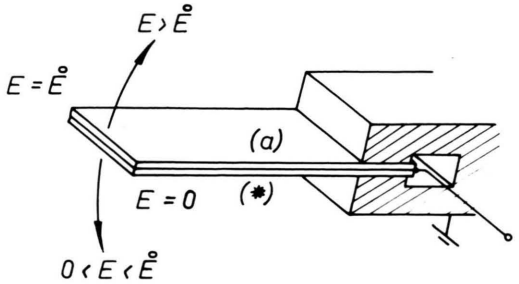

Fig. 13. Illustration of the proposed bimorph and its action.

by Uchino [21] it could be used in "digital" displacement devices. Contrary to the anti-ferroelectric material discussed by Uchino, such materials have the advantage of sharp longitudinal deformation jumps and permit the exploitation of the multilayer technique.

The use of the bistable switching can easily be explained. If, for example, at 128 K an electric bias field of about 3.5 kV/cm is applied, the deformation state can be switched by small pulses of about 1.5 kV/cm. Depending on the sign of the impulse (is it the same as before or the opposite one) the deformation remains constant or jumps up respectively down. At lower temperatures (see e.g. 118 K) no bias field but higher pulses of about 3 kV/cm are necessary to realize such a mechanism. The predicted deformation jump could be in a range of about 10^{-3}.

Of course, the discussed temperature range excludes practical application but a continued search could reveal better materials.

Finally, a third example shall be mentioned. If a material with an electrostrictive strain-field dependence like that marked by (*) in Fig. 12 (observed e.g. in PLZT ceramics or in $BaTiO_3$) is combined with another one having a field dependence like that marked by (a) (observed e.g. in BTS-13 [22] or (b), a bimorph can be build up (Fig. 13) which facilitates the zero position (no bending) at two field values (zero and $\mathring{E}$). A small deviation from $\mathring{E}$ bends the bimorph up or down depending on the direction of the deviation.

The presented method permits the selection of suited materials with respect to the above discussed as well as other applications. It helps to create and develop future actuators and devices of the coming microelectromechanical generation especially on the basis of electrostrictive materials.

[1] J. von Cieminski, Z. Naturforsch. **45a,** 1090 (1990).
[2] G. Schmidt, G. Borchhardt, J. von Cieminski, D. Grützmann, E. Purinsch, and V. A. Isupov, Ferroelectrics **42,** 3 (1982).
[3] J. von Cieminski, G. Schmidt, V. K. Magatayev, V. F. Glushkov, and L. A. Shuvalov, Ferroelectrics Letters **3,** 163 (1985).
[4] G. A. Smolenskiy, J. Phys. Soc. Japan **28,** Suppl., 26 (1970); Proc. II. Int. Meeting on Ferroelectricity 1969.
[5] G. Schmidt, Z. Physik **145,** 534 (1956).
[6] A. F. Devonshire, Adv. Physics **3,** 102 (1954).
[7] K. Roleder, J. Phys. E. Sci. Instrum. **16,** 1157 (1983).
[8] W. Pan, Q. Zhang, A. S. Bhalla, and L. E. Cross, J. Amer. Ceram. Soc. **71,** C-302 (1988).
[9] I. S. Sheludev, Electric Crystals, Nauka, Moscow 1969.
[10] M. E. Caspari and W. J. Merz, Phys. Rev. **80,** 1082 (1950).
[11] W. P. Mason, Piezoelectric Crystals and their Application to Ultrasonics, Van Nostrand, Toronto 1950.
[12] C. J. Johnson, Appl. Phys. Lett. **7,** 221 (1965).
[13] W. J. Merz, Phys. Rev. **91,** 513 (1953).
[14] G. Schmidt and P. Pfannschmidt, phys. stat. sol. **3,** 2215 (1963).
[15] C. Pawlaczyk, Wissenschaftliche Beiträge, KTB-MLU **39(05),** 29 (1978).
[16] H. M. Choe, J. H. Judy, and A. van der Ziel, Ferroelectrics **15,** 181 (1977).
[17] H. Arndt, Wiss. Z. Univ. Halle XXXV '86 M, H. 1, 18 (1986).
[18] K. Hamano and T. Shinmi, J. Phys. Soc. Japan **33,** 118 (1972).
[19] T. Mori and H. Tamura, J. Phys. Soc. Japan **19,** 1247 (1964).
[20] T. A. Pikka and V. M. Fridkin, Fiz. Tverd. Tela **10,** 3378 (1968).
[21] K. Uchino, Amer. Cer. Soc. Bull. **65,** 647 (1986).
[22] J. von Cieminski, H. T. Langhammer, and P. Abicht, submitted to phys. stat. sol.